Two Residues of a Conserved Aromatic Ladder of the Mitochondrial ADP/ATP Carrier Are Crucial to Nucleotide Transport

ARTICLE *in* BIOCHEMISTRY · JANUARY 2009

Impact Factor: 3.02 · DOI: 10.1021/bi8012565 · Source: PubMed

7 AUTHORS, INCLUDING:

Guy Jean-Marie Lauquin
French National Centre for Scientific Resea…
107 PUBLICATIONS **3,079** CITATIONS

SEE PROFILE

Two Residues of a Conserved Aromatic Ladder of the Mitochondrial ADP/ATP Carrier Are Crucial to Nucleotide Transport†

Claudine David,‡ Bertrand Arnou,‡,§ Jean-Frédéric Sanchez,‡ Ludovic Pelosi,|| Gérard Brandolin,|| Guy J.-M. Lauquin,‡ and Véronique Trézéguet*,‡

Laboratoire de Physiologie Moléculaire et Cellulaire, Institut de Biochimie et Génétique Cellulaires, UMR 5095, CNRS-Université Bordeaux 2, 1, rue Camille Saint-Saëns, F-33077 Bordeaux Cedex, France, and Laboratoire de Biochimie et Biophysique des Systèmes Intégrés (LBBSI), Institut de Recherches en Technologies et Sciences du Vivant (iRTSV), UMR 5092, CNRS-CEA-Université Joseph Fourier, F-38054 Grenoble Cedex 9, France

Received July 4, 2008; Revised Manuscript Received October 24, 2008

ABSTRACT: The mitochondrial ADP/ATP carrier is the paradigm of the mitochondrial carrier family (MCF), whose members are crucial for cross-talks between mitochondria, where cell energy is mainly produced, and the cytosol, where cell energy is mainly consumed. These carriers share structural and functional characteristics. Resolution of the 3D structure of the beef mitochondrial ADP/ATP carrier, in a complex with one of its specific inhibitors, revealed interesting features and suggested the involvement of some particular residues in substrate binding and transfer from the outside to the inside of mitochondria. To ascertain the role of these residues, namely, Y186, Y190, F191, and Y194, they were mutated into alanine in the yeast mitochondrial ADP/ATP carrier at equivalent positions (Y203, Y207, F208, and Y211). Two residues, Y203 and F208, appeared to be crucial for transport activity but not for substrate binding *per se*, indicating their involvement in the substrate transfer process through the carrier. Furthermore, it was possible to show that these mutations precluded conformational changes of the matrix loop m2, whose movements were demonstrated to participate in substrate transport by the wild-type carrier. Therefore, these aromatic residues may be involved in substrate gliding, and they may also confer specificity toward adenine nucleotides for the ADP/ATP carrier as compared with the MCF members.

The three-dimensional structure of the bovine mitochondrial adenine nucleotide carrier (BAncp),[1] a model member of the mitochondrial carrier family (MCF), has been solved by X-ray crystallography at 2.2 Å resolution (*1*). The structure is that of a monomer in complex with carboxyatractyloside (CATR), a highly specific inhibitor of Ancp to which it binds with very high affinity. Ancp has the general shape of a basket delineated by six tilted transmembrane segments (TMS 1−6).

It has been postulated on the basis of numerous biochemical data that Ancp changes its conformation to perform nucleotide transport (ref *2* and references therein). The conformation deciphered by X-ray analyses opens to the intermembrane space (IMS). Bongkrekic acid (BA) and isoBA are the second class of inhibitors that are very specific to Ancp. They bind with very high affinity but only to the matrix side of the carrier, in contrast to CATR and ATR (the decarboxylated form of CATR), which bind only to the IMS side. ATR and CATR prevent transport of ADP added on the cytosolic side, and biochemical studies have suggested that ATR/CATR and nucleotide binding sites partially overlap (*3*). Therefore, and given that Ancp transports only the magnesium-free forms of ADP and ATP (*4, 5*), analyses of residues located in the Ancp cavity suggest the mechanism of nucleotide binding, at least from the IMS side, and translocation.

In the following, numbering of BAnc1p amino acid residues starts after the initiating methionine, and numbering of ScAnc2p starts at the initiating methionine to avoid renumbering of already characterized mutations of this carrier (for example, R96H of *op1* (*6*)). Basic residues at the entrance of the cavity (K22, R79, and R279 of the bovine Anc1p or BAnc1p) may attract nucleotides that would glide further with their adenine ring along a "tyrosine ladder" (Y186, Y190, and Y194 in TMS 4) to reach a second patch of basic residues (K32, R137, and R234) (*1, 7*). These six basic residues are very well conserved in the 116 known

† This work was supported by the University of Bordeaux 2, the Centre National de la Recherche Scientifique, and the Région Aquitaine. B.A. was supported by the French Ministère de l'Enseignement Supérieur et de la Recherche. J.-F.S. was awarded a grant from the Fondation pour la Recherche Médicale.

* To whom correspondence should be addressed. E-mail: vero.trezeguet@ibgc.u-bordeaux2.fr. Phone: (33) 556 99 90 39. Fax: (33) 556 99 90 63.

‡ CNRS-Université Bordeaux 2.

§ Present address: CEA, iBiTecS (Institut de Biologie et Technologies de Saclay), CNRS, URA 2096, Université Paris-Sud 11, LRA 17V, F-91191 Gif-sur-Yvette, France.

|| CNRS-CEA-Université Joseph Fourier.

[1] Abbreviations: *ANC*, mitochondrial adenine nucleotide carrier (ADP/ATP carrier) encoding gene; Ancp, adenine nucleotide carrier (ADP/ATP carrier); ATR, atractyloside; BAnc1p, isoform 1 of bovine Ancp; BA, bongkrekic acid; EMA, eosin-5-maleimide; IMS, intermembrane space; MCF, mitochondrial carrier family; MIM, mitochondrial inner membrane; N-ADP, naphthoyl-ADP; Sc, *Saccharomyces cerevisiae*; ScAnc2p, isoform 2 of *Saccharomyces cerevisiae* Ancp; SDS−PAGE, sodium dodecyl sulfate−polyacrylamide gel electrophoresis; TMS, transmembrane segment; YPD, rich yeast extract peptone dextrose medium.

10.1021/bi8012565 CCC: $40.75
Published on Web 11/17/2008

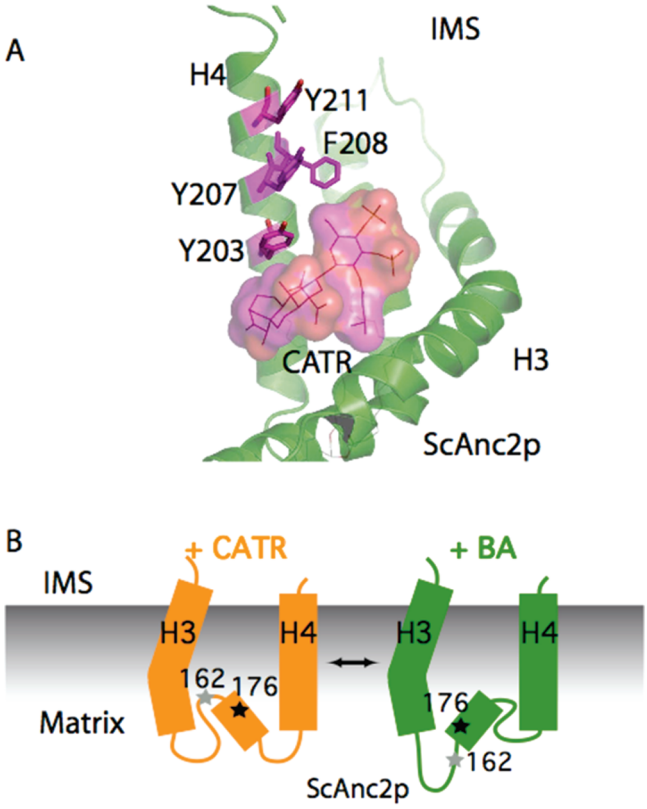

FIGURE 1: (A) Modeling of the ScAnc2p 3D structure in complex with CATR. A 3D model of Anc2p from *S. cerevisiae* based on the template structure of BAnc1p (PDB entry 1okc (*1*)) was constructed as indicated in Materials and Methods. Only part of TMS 3 and 4 (H3 and H4) are represented. The carboxyatractyloside ligand was inserted using the docking program AutoDock3. The "tyrosine ladder" described in the beef Anc1p 3D structure corresponds to residues Y186, Y190, and Y194 to which F191 is added to constitute the "aromatic ladder", corresponding to Y203, Y207, F208, and Y211 of ScAnc2p. CATR = carboxyatractyloside. (B) Movements of the matrix loop m2 upon inhibitor binding (from ref *14*). Only transmembrane helices 3 and 4 and the small helix h34 of the matrix loop m2 are represented. The stars represent residues 162 (gray) and 176 (black). Serine 162 was mutated into a cysteine in ref *14*, and V176 was mutated into cysteine in this study. Numbering of ScAnc2p amino acid residues starts at the initiating methionine and thus corresponds to numbering of the gene codons. In ref *14*, S162 is numbered S161 since amino acid numbering in this paper corresponds to that of the mature protein whose initiating methionine has been removed (*20*).

Ancp amino acid sequences (*8*). Their mutations at equivalent positions of ScAnc2p into alanine or isoleucine inactivate mitochondrial function in yeast (*9*−*12*). Next to Y190 of the BAnc1p lies F191, which is perfectly conserved in all known Ancp sequences. Therefore, the "tyrosine ladder" is renamed the "aromatic ladder" and consists of Y186, Y190, F191, and Y194 of BAnc1p. We showed in a previous study that in ScAnc2p the double replacement of Y203 (equivalent to Y186) and Y207 (equivalent to Y190) with alanine strongly impaired yeast growth on nonfermentable carbon sources while replacement with phenylalanine did not (*1*).

To assess more precisely the role of the aromatic ladder residues located in the C-terminal end of TMS 4 in nucleotide gliding during transport, they were sequentially replaced with alanine either one at a time or in pairs in ScAnc2p (Y203, Y207, F208, and Y211, Figure 1A). ATR binding properties were determined with isolated mitochondria, as well as nucleotide binding, which was examined using of a non-transportable ADP analogue, 3′-*O*-(1-naphthoyl)adenosine 5′-diphosphate (N-ADP). The results suggest that the aromatic patch residues are not involved in nucleotide binding *per se* but rather in substrate gliding via conformational changes in ScAnc2p.

We have then generated a cysteine-less variant of ScAnc2p (Anc2CLp) into which a single cysteine residue was introduced at position 176 (Anc2CLp^{V176C}) located in the small α-helix of the matrix loop m2 at a position equivalent to C159 of BAnc1p (Figure 1A). Indeed, movements of the matrix loop m2 during nucleotide transport have been revealed from various experimental approaches: limited proteolysis (*13, 14*), chemical labeling of SH groups (*15*−*17, 14*), and photolabeling of the carrier with photoactivatable analogues of atractyloside and adenine nucleotides (*18*−*20*). It was proposed that the N-terminal part of m2 is accessible from the IMS and that the C-terminal part is exposed to the mitochondrial matrix in the Ancp•CATR complex ("CATR" conformation) (Figure 1B). Conversely, in the Ancp•BA complex, the C-terminal part of m2 is accessible from the IMS, and the N-terminal part is exposed to the matrix ("BA" conformation) (Figure 1B) (*14*).

The single cysteine variant Anc2CLp^{V176C} is active. EMA labels V176C in the absence or in the presence of ADP or BA. In contrast, CATR prevents this labeling, suggesting that large conformational changes of the matrix loop m2 may take place upon ligand binding. The Y203A and F208A mutations were introduced into Anc2CLp^{V176C} (Anc2CLp^{V176CY203A} and Anc2CLp^{V176CF208A}), and these variants were never labeled with EMA, whatever the added ligand, indicating that the Y203A and F208A mutations might preclude some of the conformational changes essential for ADP/ATP transport, thus pointing to the role of these residues in nucleotide gliding.

MATERIALS AND METHODS

Chemicals. [^{3}H]Atractyloside ([^{3}H]ATR) and 3′-*O*-(1-naphthoyl)adenosine 5′-diphosphate (N-ADP) were synthesized as previously described (*21, 22*). Protein concentration was determined using the bicinchoninic acid reagent kit from Sigma. Nucleotides and CATR were purchased from Sigma, and P_1,P_5-di(adenosine-5′)-pentaphosphate was from Calbiochem. Hexokinase/glucose-6-phosphate dehydrogenase enzyme mix was obtained from Roche Diagnostics GmbH.

Strains, Media, and Transformation. Escherichia coli strain used for plasmid propagation was XL1-Blue (*recA1 endA1 gyrA96 (Nal^r) thi hsdR17 (r_K^- m_K^+) supE44 relA1 lac$^-$ F′ [Tn10 (tet^r) proAB$^+$ lacI^q lacZΔM15]*). Bacteria were transformed according to standard methods either with calcium chloride or by electroporation, as already described (*23*). The following *Saccharomyces cerevisiae* strains were used in this study: *JL1Δ2Δ3u*$^-$ (*MATα leu2-3,112 his3-11,15 ade2-1 trp1-1 ura3-1 can1-100 anc1::LEU2 Δanc2::HIS3 Δanc3*) (this work); *JL1-3ANC2* (*MATα leu2-3,112 his3-11,15 ade2-1 trp1-1 ura3-1 can1-100 anc1::LEU2 anc3::URA3*) which refers to the *2N1-3* strain (*24*). The *JL1Δ2Δ3u*$^-$ strain was obtained after replacement by homologous recombination of the interrupted *anc3* gene of *JL1-3Δ2* (*23*) with a fragment corresponding to the deletion of *ScANC3* nucleotides +269 (*Hin*dIII site) to +975 (*Cla*I site), the STOP codon being at position +922. This fragment contained 48

bp of the 5′ noncoding region of *ScANC3* followed by the first 269 bp of the *ScANC3* sequence and 324 bp of the 3′ noncoding region (from the *Cla*I site to the *Bam*HI site of the *ScANC3* gene). Removal of the *URA3* gene in the *anc3* locus was controlled by the ability of the recombinant strain to grow in the presence of 5-fluoroorotic acid (*25*).

The strains were cultivated and transformed as described in ref *23*. The composition of all the media used (YPD, YPLact, SGal-W) is described in ref *23*.

Site-Directed Mutagenesis. Site-directed mutagenesis of *ScANC2* was performed using the Transformer site-directed mutagenesis kit (Clontech Laboratories) with the following mutagenic primers (mutated bases are underlined and amino acid substitution is indicated in parentheses): ^{598}5′-ATTGTTGTCGCTAGAGGTCTATACTTCGGTATGTACG-3′^{634} (Y203A), ^{598}5′-ATTGTTGTCTACAGAGGTCTAGCTTTCGGTATGTACG-3′^{634} (Y207A), ^{598}5′-ATTGTTGTCTACAGAGGTCTATACGCTGGTATGTACG-3′^{634} (F208A), ^{619}5′-TACTTCGGTATGGCTGATTCTTTGAAG-3′^{645} (Y211A), ^{598}5′-ATTGTTGTCGCTAGAGGTCTAGCTTTCGGTATGTACG-3′^{634} (Y203A, Y207A), ^{598}5′-ATTGTTGTCTACAGAGGTCTAGCTGCTGGTATGTACG-3′^{634} (Y207A, F208A), ^{206}5′-GTATCTTAGACGCTTTCAAGAGAACCGC-3′^{233} (C73A), ^{718}5′-GGTGCTTCTACAGCTTCTTACCCATTGG-3′^{744} (C244A), ^{799}5′-GGTGCCTTTGACGCTTTGAGGAAGATTG-3′^{826} (C271A), ^{850}5′-CTATTCAAGGGTGCTGGTGCTAACATC-3′^{876} (C288A), and ^{513}5′-CGGTTTGATCGATTGCTACAAGAAGACC-3′^{540} (V176C).

The mutated *ScANC2* genes were subcloned into a centromeric plasmid, pRS314, under the control of *ScANC2* regulatory sequences as described in ref *23*. The resulting plasmids were used to transform the *JL1*Δ*2*Δ*3u*$^-$ strain to assess their ability to complement the *Scanc2* deletion.

Isolation of Mitochondria, Kinetic Measurements, and Immunodetection. Yeast cells used for isolation of mitochondria were grown in minimal synthetic medium consisting of 0.17% yeast nitrogen base without amino acids and ammonium sulfate, 0.5% $(NH_4)_2SO_4$, 2% galactose, and all amino acids except tryptophan (SGal-W) to allow the plasmid to be maintained in transformants. The protocols and materials used to perform isolation of mitochondria, ADP/ATP transport, [^{3}H]ATR binding measurements, and protein immunostaining are described in ref *23*. Free ADP concentrations were calculated using WEBMAXC STANDARD (http://www.stanford.edu/~cpatton/webmaxc/webmaxcS.htm). After ECL detection with a GENE GNOME system (Syngene, Ozyme), signal intensities of the bands were quantified with Genetools, a Syngene software. The time course of CATR-induced release of bound 3′-*O*-(1-naphthoyl)adenosine 5′-diphosphate (N-ADP) binding was studied by incubating freshly isolated mitochondria in 2 mL of 120 mM KCl, 10 mM MOPS, pH 6.8, and 1 mM EDTA at 16 °C (0.5 mg of mitochondrial proteins/mL). After N-ADP addition (from 0.1 to 10 μM) the fluorescence level was set to zero. Then the increase in fluorescence induced upon addition of 5 μL of 2 mM CATR (ΔF) was recorded until it became stable. The apparent dissociation constant, $K_{1/2}$, was determined after plotting $\Delta F/\Delta F_{max}$ as a function of added N-ADP concentration.

EMA Labeling of Membrane-Embedded ScAnc2p Variants. Mitochondria were isolated in buffer A (0.6 M mannitol, 10 mM Tris·HCl, 0.1 mM Na_2EGTA, pH 7.4), resuspended in buffer B (0.6 M mannitol, 10 mM MOPS, 0.1 mM Na_2EGTA, pH 6.8) at 8 mg of proteins/mL (final concentration), and incubated for 15 min at 4 °C in the absence or in the presence of 20 μM CATR or 20 μM BA. They were then diluted twice with buffer A and incubated in the dark for 30 min at 4 °C in the presence of 200 μM EMA. Labeling was stopped by 20 mM DTT (10 min, 4 °C, in the dark). After addition of 1 volume of 2× electrophoresis sample buffer (125 mM Tris·HCl, pH 6.8, 20% glycerol, 4% SDS, 0.2% 2-mercaptoethanol, 0.001% bromophenol blue), samples were incubated for 2 min at 70 °C and then loaded on a 20% polyacrylamide gel (SDS−PAGE). After migration, fluorescence was detected at λ_{ex} = 532 nm with the fluorescent image analyzer Fujifilm FLA-500.

Construction of a Three-Dimensional Model Structure for ScAnc2p. A pairwise alignment between ScAnc2p and bAnc1p sequences was constructed using ClustalX (*26*), and manual refinement was based on multiple sequence alignment of 116 Ancp sequences generated with ClustalX. A three-dimensional model of ScAnc2p was built using the homology modeling program Modeller (*27*) and the template structure of bAnc1p (PDB entry: 1okc). We used the AutoDock 3.05 package (*28*) for ligand docking. The CATR structure was generated using the prodrg server (http://davapc1.bioch.dundee.ac.uk/prodrg/ (*29*)) and AutoDockTools program (*30*). Blind docking was carried out using the Lamarckian genetic algorithm for 512 trials and with a rmsd tolerance of 0.5 Å for clustering and 2 Å for reclustering.

RESULTS

Growth Phenotypes on a Nonfermentable Carbon Source Suggest Differing Involvement of the Aromatic Ladder Residues. Y186 of the BAnc1p aromatic ladder is conserved in 100% of the Ancp amino acid sequences, Y190 in 98%, F191 in 100%, and Y194 in 87%. In the remaining cases they are replaced with phenylalanine, another aromatic amino acid (*8*). Mutation of Y203 and Y207 of ScAnc2p (equivalent to Y186 and Y190 of BAnc1p) (Anc2p^{Y203FY207F}) into phenylalanine did not prevent *JL1*Δ*2*Δ*3u*$^-$ growth on nonfermentable carbon sources (Figure 2, line 3) but conferred cold sensitivity on lactate. In contrast, when both residues were mutated simultaneously into alanine (Anc2p^{Y203AY207A}), yeast growth on nonfermentable carbon sources was impaired (Figure 2, line 4, and ref *1*), and the transformants were temperature (12 and 37 °C) sensitive on glucose (data not shown). Thus, one or both of these residues may play a crucial role in nucleotide transport.

The role of the aromatic ladder was further investigated by mutating the four residues of ScAnc2p into alanine, in pairs or one at a time, namely, Y203, Y207, F208, and Y211. Introduction of two alanines simultaneously prevented growth on lactate at 28 °C (Figure 2, lines 4−6) and conferred temperature sensitivity on glucose (data not shown). Mutation into alanine of one residue at a time clearly showed that Y207 was dispensable to ScAnc2p function (Figure 2, line 8), in contrast to Y203 and F208. Indeed, ScAnc2p^{Y203A} and ScAnc2p^{F208A} strains exhibited a growth defect on lactate at 28 °C (Figure 2, lines 7 and 9) and 12 or 37 °C (not shown), while the ScAnc2p^{Y211A} strain displayed a reduced growth phenotype at 28 °C (Figure 2, line 10) and no growth at 12 or 37 °C (not shown).

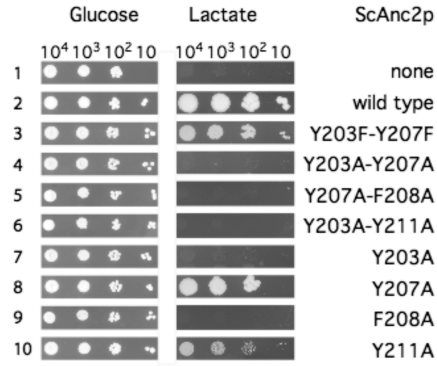

FIGURE 2: Yeast growth phenotype associated with aromatic ladder residue mutations. *JL1*Δ*2*Δ*3u*$^-$ strain was transformed with plasmid pRS314 containing no gene (line 1), the wild-type *ScANC2* gene (line 2), or the various *Scanc2* mutated genes (lines 3−10), under the control of *ScANC2* regulating sequences. Yeast transformants were isolated and inoculated in liquid complete minimum medium free of tryptophan containing 2% glucose as carbon source (SC-W). When the cultures reached log phase, cells were diluted to obtain 10^4, 10^3, 10^2, or 10 cells per 2 μL and then spotted onto SC-W (glucose) or rich lactate-containing medium (lactate) plates and incubated at 12, 28, or 37 °C. For the sake of clarity, only results obtained after 3 days (glucose) or 6 days (lactate) of incubation at 28 °C are shown.

All Variant Genes Lead to ScAnc2p Production in Mitochondria. In the cases of ScAnc2p^{Y203A} and ScAnc2p^{F208A} variants, the lactate minus growth phenotype might reflect the lack of ScAnc2p variants in mitochondria should these proteins be unstable either before or after their insertion into MIM. Amounts of carrier proteins in mitochondria were first evaluated from immunostaining experiments. Ten micrograms of proteins from mitochondria isolated from *JL1*Δ*2*Δ*3u*$^-$ transformed with the plasmids encoding the variants was loaded on a 12% acrylamide gel. After SDS−PAGE and transfer, the nitrocellulose membrane was first immunostained with an antibody raised against the last 14 amino acids of ScAnc2p (1/10000) (*31*). After ECL detection, the membrane was immunodecorated with an antibody raised against yeast porin (1/10000) (*32*). The signal intensities were quantified and plotted as ScAnc2p/porin ratios (Figure 3). ScAnc2p was present in every transformant, but its relative amount varied with the variant. The relative amounts of the more active variants, ScAnc2p^{Y203FY207F} and ScAnc2p^{Y207A}, were similar to that of the wild type, whereas ScAnc2p^{Y211A} and the inactive forms were less abundant. Importantly, however, all of the variant transporters, even the inactive ones, were present in mitochondria in reasonable amounts.

To quantify ScAnc2p variants more precisely, we performed [^{3}H]ATR binding experiments with isolated mitochondria. Results are given in Table 1 and roughly correlate with those of Figure 3, when considering the maximum number of binding sites (B_{max}^{ATR}) for two variants, ScAnc2p^{F208A} and ScAnc2p^{Y211A}. However, they were quite different for ScAnc2p^{Y203A} and ScAnc2p^{Y207A}. The B_{max}^{ATR} values were higher than that of the wild type whereas the relative amounts as evidenced by immunodecoration were lower (ScAnc2p^{Y203A}) or similar (ScAnc2p^{Y207A}).

ATR binding experiments may be used to estimate the absolute amount of properly folded ScAnc2p in mitochondria while immunodecoration indicates only the amount of ScAnc2p relative to porin. The greatest divergence was

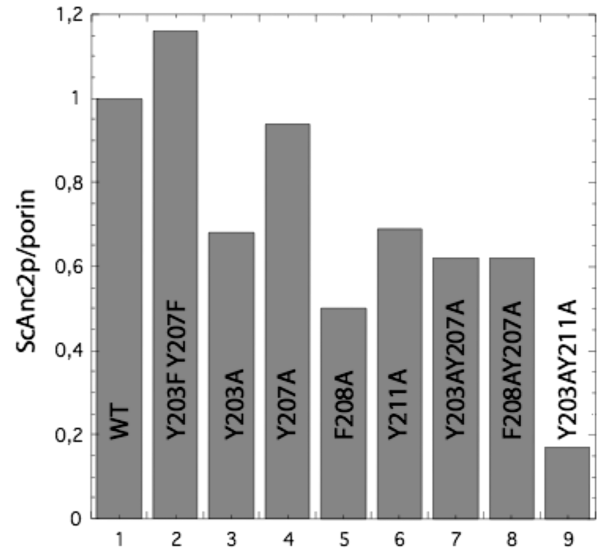

FIGURE 3: Relative ScAnc2p content determined after immunostaining of mitochondria proteins. Mitochondria were isolated from cells grown in SGal-W. Ten micrograms of mitochondrial proteins was subjected to SDS−PAGE and transferred onto nitrocellulose membrane which was then immunodecorated with an antibody raised against the last 14 amino acids of ScAnc2p (1/10000) and then with an antibody raised against yeast porin (1/10000). Intensities of the signals were quantified with GeneTools from Syngene after each revelation. The ratio ScAnc2p/porin in arbitrary units was set at 1 for the wild-type protein. Data are the means of two different experiments.

Table 1: [^{3}H]ATR Binding Parameters and Naphthoyl-ADP Dissociation Constants

	ATR binding[b]		N-ADP binding
ScAnc2p variant	B_{max}^{ATR} (pmol/mg)	K_D^{ATR} (nM)[b]	$K_{1/2}$ (μM)[c]
WT[a]	337 ± 27	327 ± 26	1.7 ± 0.4
R96H (*op1*)[a]	445 ± 236	226 ± 116	nd[d]
Y203A	392 ± 21	2002 ± 245	2.6 ± 0.2
Y207A	637 ± 85	177 ± 35	nd
F208A	264 ± 9	68 ± 12	1.8 ± 0.2
Y211A	211 ± 12	45 ± 13	nd

[a] From ref *33*. [b] Various [^{3}H]ATR concentrations were incubated with isolated mitochondria (1 mg). After incubation on ice (45 min), mitochondria were pelleted, washed, and lyzed with 5% Triton X-100 and 0.5 M NaCl. Radioactivity associated with the pellet was counted to calculate the amount of [^{3}H]ATR bound to mitochondria. Nonspecific binding was measured in the presence of 500 μM CATR. B_{max}^{ATR} = number of maximum ATR binding sites. [c] Various concentrations of N-ADP were added to isolated mitochondria (0.5 mg/mL). The fluorescence level was set to zero. Addition of CATR released N-ADP from mitochondria inducing an increase in fluorescence (ΔF). The $K_{1/2}$ value was determined by plotting $\Delta F/\Delta F_{max}$ as a function of added N-ADP. [d] nd, not determined.

observed with the active variant ScAnc2p^{Y207A}. This could mean that, in cells expressing this variant, the amount of mitochondrial proteins is modified.

Some of the ATR dissociation constant values were dramatically changed. They decreased by a factor of 5−7 for the ScAnc2p^{F208A} and ScAnc2p^{Y211A} variants, while they increased by a factor of 6 for the ScAnc2p^{Y203A} variant. This suggests a large decrease in ATR affinity for the latter, which could correlate with a decrease in nucleotide binding ability. Indeed, numerous studies have suggested overlapping of ATR and ADP binding sites, at least partially.

Some of the Rungs of the Aromatic Ladder Are Crucial to Nucleotide Translocation or Binding. In a previous paper we showed that the *op1* mutation of ScAnc2p (R96H),

Table 2: ADP/ATP Exchange Parameters

ScAnc2p variant	V_{max}^{ADP} (nmol min^{-1} mg^{-1})	K_M^{ADP} (μM)	doubling time[c]
WT[a]	90 ± 3	0.68 ± 0.08	3 h 30 min
R96H (*op1*)[a]	94 ± 8	368 ± 66	
Y203F Y207F	94 ± 6	9 ± 2	7 h 30 min
Y203A	81 ± 6	328 ± 61	
Y207A	78 ± 2	0.9 ± 0.1	6 h
F208A	NM[d]	NM	
Y211A	54 ± 1	8.5 ± 0.8	17 h 30 min
V176C[b]	47 ± 1	1 ± 0.2	4 h 30 min

[a] From ref *33*. [b] Corresponding to Anc2CLp^{V176C}. [c] Doubling time was determined by measuring at various time intervals the absorbance at 600 nm of yeast cells cultivated in YPlact. [d] NM, not measurable.

though impairing yeast growth on a nonfermentable carbon source, did not modify the maximum rate of ADP/ATP exchange but rather the K_M for external ADP (*33*), whose value was increased about 500-fold as compared to the wild-type protein. It was therefore of crucial importance to determine whether Y203A and F208A mutations had similar effects on ScAnc2p activity. We measured ADP/ATP exchange kinetic parameters with mitochondria isolated from the strains expressing the corresponding variants. Results are given in Table 2. Interestingly, ScAnc2p^{Y203A} behaved similarly to the *op1* mutant: the V_{max}^{ADP} value was similar to that of the WT, but the K_M^{ADP} value was increased almost 500-fold. In contrast, ScAnc2p^{Y207A}, which grew on lactate, had a K_M^{ADP} value similar to that of WT and a slightly decreased V_{Max}^{ADP} value. The ScAnc2p^{F208A} variant could not perform ADP/ATP exchange. The ScAnc2p^{Y211A} variant had a decreased V_{max}^{ADP} value (around 2-fold) and an increased K_M^{ADP} value (12.5-fold) but not as much as ScAnc2p^{Y203A}, accounting for the reduced but still significant growth observed on lactate (Figure 2, line 10).

The Aromatic Ladder Is Not Crucial to ADP Binding per se. 3′-*O*-(1-Naphthoyl)adenosine 5′-diphosphate (N-ADP) is a nontransportable ADP analogue whose binding properties to Ancp can be examined with isolated mitochondria (*22*). Its fluorescence is quenched upon binding to Ancp, so specific binding to the mitochondrial Ancp can be measured by the fluorescence enhancement observed upon dissociation after addition of CATR, a very specific Ancp inhibitor. The $K_{1/2}$ value of N-ADP binding to the beef Ancp is 3 μM (*22*), which is close to the value determined for the yeast ScAnc2p ($K_{1/2}$ = 1.7 μM, Table 1). As can be seen in Table 1, the $K_{1/2}$ values are in the same range for ScAnc2p^{Y203A} and ScAnc2p^{F208A}, which are inactive for transport (2.6 and 1.8 μM, respectively). This suggests that the absence of nucleotide transport catalyzed by these variants does not result from their inability to bind nucleotides but rather from their inability to catalyze the substrate translocation step.

The m2 Loop of ScAnc2p^{Y203A} and of ScAnc2p^{F208A} Is Locked in a "CATR"-like Conformation. CATR and BA are known to induce conformational changes similar to those involved in nucleotide translocation during which the matrix loop m2 plays an important role. C159 of BAnc1p in the middle of loop m2 was differentially labeled by the non-permeant sulfhydryl-alkylating reagent eosin-5-maleimide (EMA) in the presence or absence of nucleotides, CATR or BA (*15*). This labeling inhibited ADP/ATP transport. C159 corresponds to V176 of the yeast ScAnc2p, which nonetheless contains four cysteinyl residues: C73 in matrix loop m1

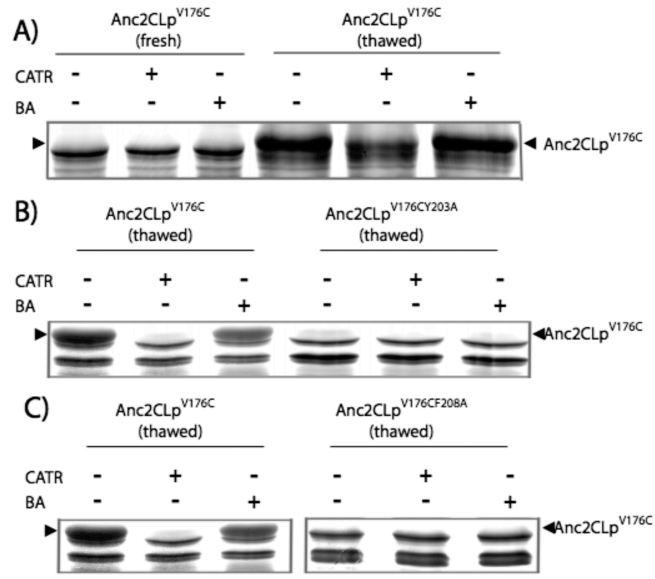

FIGURE 4: (A) EMA labeling of the membrane-bound Anc2CLp^{V176C} variant in mitochondria. Freshly isolated mitochondria or frozen−thawed mitochondria were incubated (8 mg of proteins/mL) without or with 20 μM CATR or 20 μM BA for 15 min on ice. EMA labeling (200 μM) was performed for 30 min on ice in the dark. The reaction was stopped with 20 mM DTT. Samples were subjected to SDS−PAGE, and fluorescence was visualized at λ_{ex} = 532 nm. The position of Anc2CLp^{V176C}, indicated by an arrow, was controlled by immunoblotting after transfer of the gel onto a nitrocellulose membrane. The EMA-labeled bands, which migrated in the gels immediately ahead of the Anc2p band, have been tentatively identified to the phosphate carrier and the mitochondrial porin (VDAC1) according to refs *44* and *14*. (B, C) Y203A (B) and F208A (C) prevent EMA labeling of the membrane-bound Anc2CLp^{V176CY203A} (B) and Anc2CLp^{V176CY203A} (C). Frozen−thawed mitochondria (8 mg of proteins/mL) containing Anc2CLp^{V176C} (B and C), Anc2CLp^{V176CY203A} (B), or Anc2CLp^{V176CF208A} (C) were incubated without or with 20 μM CATR or 20 μM BA for 15 min on ice. EMA labeling was performed as indicated in panel A.

(equivalent to C56 of BAnc1p), C244 in TMS 5, C271 in matrix loop m3 (equivalent to C256 of BAnc1p), and C288 in the C-terminal end of m3. None of them was labeled with EMA in the wild-type ScAnc2p embedded in mitochondrial membrane (ref *14* and data not shown). We first engineered a mutant of ScAnc2p in which the four endogenous cysteinyl residues were mutated into alanine (Anc2CLp). We then mutated V176 in order to introduce a cysteine in the matrix loop m2, at a position equivalent to that of C159 of BAnc1p (Anc2CLp^{V176C}) (Figure 1A). Such a mutation does not preclude yeast growth on a nonfermentable carbon source, and its doubling time in rich lactate-containing medium is approximately 4 h 30 min, which is comparable to that of the wild-type cells (3 h 30 min (*23*)). Furthermore, Anc2CLp^{V176C} exchanged nucleotides with a significant efficacy since the K_M^{ADP} value was in the same range though the V_{max} value was half that of the wild type (Table 2). Last, we controlled that the Anc2CLp^{V176C} protein was stable over the EMA labeling duration by Western blot analyses of mitochondria at the end of the labeling experiments (data not shown).

EMA labeling was performed with freshly isolated and with frozen−thawed mitochondria in the absence or in the presence of CATR or BA. As can be seen in Figure 4A (lanes 1−3), Anc2CLp^{V176C} was never labeled with EMA in freshly isolated mitochondria. However, it was labeled in thawed

mitochondria in the absence of ligand, and this labeling was inhibited by preincubation of mitochondria with CATR but not with BA (Figure 4A, lanes 4−6). Therefore, V176C EMA labeling appears to be a good reporter of carrier conformational changes induced by inhibitor binding, though at this stage we cannot exclude that CATR prevents EMA labeling only by steric hindrance. This point is discussed below. The difference between freshly isolated or thawed mitochondria can be accounted for by rupture of the outer and/or the inner membrane that would give EMA access to Anc2p.

Since the affinity of ScAnc2p^{Y203A} for ATR was dramatically reduced as compared to the wild-type protein, Y203 of Anc2CLp^{V176C} was mutated into alanine, and EMA labeling was examined for this new variant. As expected, the Y203A mutation precluded yeast growth on a nonfermentable carbon source. However, the new variant was stable when embedded in mitochondria, and its ADP/ATP exchange capacity was similar to that of ScAnc2p^{Y203A} (data not shown). As can be seen in Figure 4B (lanes 4−6), this variant was not labeled whatever the incubation conditions as if "BA" and "CATR" conformations were similar with respect to V176C EMA labeling. Similar results were obtained with freshly isolated mitochondria (data not shown). The Y203A variant might be locked in a "CATR"-like conformation, and this locking cannot be reversed by BA binding, probably because the matrix loop m2 cannot swing in a manner appropriate for nucleotide translocation. In addition, these results allow us to exclude that the absence of EMA labeling of V176C in the presence of CATR is due to steric hindrance.

Considering such a dramatic effect of the F208A mutation on ADP/ATP transport, it was also of interest to introduce this mutation in Anc2CLp^{V176C}. As expected, the new variant Anc2CLp^{V176CF208A} did not restore yeast growth in a lactate-containing medium though the protein was present in significant amount in mitochondria (data not shown). Anc2CLp^{V176CF208A} behaved similarly to Anc2p^{F208A} regarding nucleotide transport. Interestingly, this completely inactive mutant was never labeled with EMA (Figure 4C), similarly to Anc2CLp^{V176CY203A}. The F208A mutation might also lock ScAnc2p in a "CATR"-like conformation, which however would differ from that adopted by ScAnc2p^{Y203A} since F208A increases ATR affinity, contrary to Y203A. Furthermore, F208A completely inactivated the nucleotide transport whereas some transport was still detected with Y203A.

DISCUSSION

This paper assigns a crucial role to a structural amino acid motif initially revealed in the 3D structure of BAnc1p in complex with CATR and formerly named the "tyrosine ladder" (*1*) (Figure 1A). It was first proposed that adenine nucleotides from the IMS would be attracted and "preoriented" through the combined effect of a patch of positively charged amino acids and of the "tyrosine ladder". In this ladder, Y186 constricts the funnel-shaped cavity of BAnc1p in complex with CATR (*7*). This would restrict access of the nucleotide to the other side of the inhibited carrier, consisting of a second patch of basic and acidic residues belonging to the third signature sequence of the mitochondrial carrier family (MCF), ^{229}PFDTVR^{234} followed with ^{235}RRMMM^{239}, which is the end of the Ancp signature sequence (*7*). Right beside Y190 is F191, which is perfectly conserved in all known Ancp amino acid sequences (*8*). The orientation of its aromatic ring is almost orthogonal to that of the other tyrosyl residues (Figure 1). Thus, we hypothesized involvement of the aromatic ladder in nucleotide progress into the funnel. This was assessed by mutating the corresponding residues of yeast ScAnc2p, Y203, Y207, F208, and Y211, into alanine, in pairs or individually. Two residues, Y203 and F208, which are perfectly conserved among Ancp sequences, obviously play a crucial role in nucleotide exchange since their mutation impaired the transport function. Estimates of the variant carrier amounts in the MIM ruled out impaired Ancp variant biogenesis being responsible for the observed phenotype. However, ATR binding properties were dramatically modified for ScAnc2p^{Y203A}, in line with the observation that Y186 of BAnc1p, which is equivalent to yeast Y203, is stacked on the diterpene moiety of CATR (*1*). CATR blind docking on the 3D model of yeast Anc2p indicates that the lowest binding energy cluster corresponds to a CATR conformer located within the Ancp cavity which is open to the intermembrane space. Upon careful examination, it appears that the critical residues of ScAnc2p involved in the CATR binding, as exhibited in the crystal structure of the bAncp1·CATR complex, are also those involved in the lowest energy conformation of the CATR docking experiment. Y203, on one hand, and L142, V145, and I200, on the other, are involved respectively in stacking with the diterpene moiety of CATR and van der Waals contacts with the isovaleric residue, while N104, K108, and R204 are hydrogen-bonded to the glucose moiety of the CATR sulfate groups. In addition, R96 is involved in a salt bridge with a carboxylic group of CATR. These results indicate, first, that the analysis of our ScAnc2p mutagenesis results with the help of the bAnc1p crystal structure is perfectly relevant and, second, that the 3D model of ScAnc2p could be safely used for interpreting our results with the yeast carrier.

The loss of ring stacking loosens the Ancp·ATR complex (Table 1), which is consistent with a dramatically increased K_D^{ATR} value (Table 1). This stacking cannot be compensated for by the nearby aromatic residues, which point toward the cavity (Y207 and Y211). In the case of ScAnc2p^{F208A}, a completely inactive variant, and of ScAnc2p^{Y211A}, a less active variant, the K_D^{ATR} values are 5−7-fold lower than that of the wild type, thus indicating the formation of much more stable ScAnc2p·ATR complexes than with the wild-type ScAnc2p. F208 and Y211 are in the largest part of the cavity and oriented toward the IMS. It seems unlikely that they restrict CATR access to the cavity. Instead, they may play a role in ScAnc2p molecular "plasticity". Their mutation into alanine might lock the carrier in the "CATR" conformation, as reflected by the high affinity for ATR and by the absence of EMA labeling of V176C when associated with F208A. Aromatic residues can contribute to protein conformation through various interactions and notably through cation−π ones. Analyses of the 3D structure of BAnc1p·CATR (PDB entry: 1okc) with the CAPTURE program (*34*) identified three probable R/Y interactions that were energetically significant: R59/Y50, R104/Y111, and R234/Y131. None of them involves a residue of the aromatic ladder, though we cannot rule out this pattern as being different in the noninhibited conformation. Similar results were obtained when the presence of putative cation−π interactions was

sought within the ScAnc2p 3D model constructed by homology modeling with the BAnc1p·CATR crystal structure.

Nucleotide transport by ScAnc2p^{Y203A} or ScAnc2p^{F208A} was either dramatically impaired (Anc2p^{Y203A}) or abolished (Anc2p^{F208A}) (Table 2). The K_M^{ADP} value for ScAnc2p^{Y203A} was almost 500-fold higher than that of the WT. However, these variants can still bind a nucleotide analogue (N-ADP) with $K_{1/2}$ values similar to that of ScAnc2p (Table 1), which is puzzling at first glance. Thus the nucleotide binding step is not the main concern for these mutants but rather the nucleotide transfer from one side of the carrier to the other. This step very likely involves conformational changes. Therefore, we have introduced into ScAnc2p a cysteinyl residue in position 176 in the middle of the loop m2, which might be considered as an intrinsic conformational probe. C176 is labeled in the presence of BA but not in the presence of CATR, contrary to what is observed for Anc2CLp^{V176CY203A} and Anc2CLp^{V176CF208A}, in which C176 is never labeled, whatever the carrier inhibitor. ScAnc2p^{Y203A} and ScAnc2p^{F208A} might be locked in conformations similar to the "CATR" conformation and might be unable to swing to the "BA" conformation upon BA binding. Yet this swinging is one of the requisites of nucleotide transport, as has been shown by numerous approaches (for a review, see for example ref *8*).

Therefore, we propose that Y203 and F208, two aromatic residues of TM4 from the ScAnc2p carrier, play an essential role in nucleotide attraction and its progress through the carrier leading to a productive ADP/ATP exchange.

Our results are substantiated by two recently published papers reporting on the ADP binding on BAnc1p using a molecular dynamics approach on time scales of 0.3 (*35*) and 0.53 μs (*36*). The time scales explored are probably too short to give an insight into the conformational changes involved in the substrate translocation step. In addition, a more realistic environment mimicking the ionic composition of the IMS water phase in equilibrium with both the carrier protein and the lipid bilayer could probably contribute to a partial shielding of the electrostatic forces at work. Nevertheless, some interesting results are worth underscoring. In these studies the ADP·Ancp complex forms rapidly because of a strong electrostatic attraction between the nucleotide and the protein. The phosphate groups are attracted first, and their binding to positive conserved residues would thus trigger the conformational changes inherent to transport. In one of the simulations, adenine moiety forms successively π-stacking interactions with Y194 and Y190 (Y211 and Y207 of ScAnc2p, respectively) either individually or together (*36*). In both studies the pentose ring interacts with Y186 (Y203 of ScAnc2p) at the end of the simulation. Therefore, Y186 plays a key role in ADP transport. Interestingly, one of the simulations is abortive for ADP transport since the nucleotide remains rapidly stuck between Y194 and F191 (Y211 and F208 of ScAnc2p, respectively) (*36*). This is puzzling considering the essential role of F208 evidenced by our studies but points out to the absolute requirement of an experimental approach to corroborate molecular dynamics results.

Y203 and F208 are 100% conserved among all known Ancp sequences. A phenylalanine residue at a position equivalent to F208 is present in 71% of the MCF members of the yeast *S. cerevisiae* (Figure 5). This residue might

Consensus[1]		**Y** - - - **Y**	**F** - - **Y** - -
Locus tag[2]	*Gene name*		
YMR056c	*ANC1*	**Y** **Y**	**F** **Y**
YBL030c	*ANC2*	**Y** **Y**	**F** **Y**
YBR085w	*ANC3*	**Y** **Y**	**F** **Y**
YPR021c	*AGC1*	**F** **Y**	**F** **Y**
YPR128c	*ANT1*	P **Y**	A **F** Q
YOR100c	*CRC1*	G **Y**	**F** **Y**
YBR291c	*CTP1*	N R	L **Y**
YLR348c	*DIC1*	M Q	V **Y**
YIL134w	*FLX1*	Q **Y**	**F** **Y**
YDL198c	*GGC1*	G **F**	L **F** N **F**
YHR002w	*LEU5*	**Y** S	**F** **F** H
YJL133w	*MRS3*	**F** **F** N	**F** **Y**
YKR052c	*MRS4*	**F** **F** N	**F** **Y**
YGR257c	*MTM1*	**F** **Y**	**W** **Y**
YIL006w	*NDT1*	V **F**	P **Y** E
YEL006w	*NDT2*	V **F**	P **Y** E
YKL120w	*OAC1*	G Q	L **Y**
YPL134c	*ODC1*	**W** **Y**	**F** I **F**
YOR222w	*ODC2*	**W** **Y**	**F** I **Y**
YOR130c	*ORT1*	G **W**	**F** **Y**
YJR077c	*PIC1*	**Y** K	**F** **F**
YER053c	*PIC2*	**Y** K	**F** **F**
YBR192w	*RIM2*	G **W**	L **Y** E
YNL083w	*SAL1*	**Y** D	L **F**
YNL003c	*SAM5*	**F** Q	**F** **Y**
YJR095w	*SFC1*	N N	**F** **Y**
YGR096w	*TPC1*	T M	**F** **Y**
YDL119c	*No name*	**Y** **Y**	V **Y**
YFR045w	*No name*	N Q	**F** **Y**
YMR241w	*YHM2*	N **W** R	**F** S
YPR058w	*YMC1*	G **Y**	**F** **Y**
YBR104w	*YMC2*	G **Y**	**F** **Y**
YMR166c	*No name*	**F** Q	**F** **F** **Y**
YPR011c	*No name*	**Y** N	**F** **Y**
F %		18 6	71 9
Y %		26 38	0 65
W %		6 6	3 0
Consensus[1]		**Y** - - - **Y**	**F** - - **Y** - -
% in Ancp[3]		100 98	100 87

FIGURE 5: Sequence alignment of 34 members of *S. cerevisiae* MCF (identified or putative). (1) The aromatic ladder sequence corresponds to that defined by comparing all known Ancp sequences (*8*). The aromatic residues are in bold and italicized whatever their position. (2) The locus tags are defined in the *Saccharomyces* Genome Database (http://www.yeastgenome.org/). Sequences were aligned with ClustalX (*26*). (3) Conservation of ScAnc2p Y203, Y207, F208, and Y211 is indicated as percent of the aromatic residue at equivalent positions in the 116 Ancp sequences analyzed (*8*).

therefore also play a role in substrate transport in many carriers, regardless of substrate specificity. Y203 is much less conserved among MCF (26%) (Figure 5), and its role may be restricted to substrates bearing an adenine moiety. Indeed, it is conserved in Sal1p and Leu5p whose substrates are ATP-Mg/P_i and CoA, respectively (*37, 38*). In contrast, Ggc1p, which transports guanine nucleotides (*39*), and Rim2p, which transports pyrimidine nucleotides (*40*), contain a glycine at this position. However, the peroxisomal yeast Ant1p, which transports adenine nucleotide (*41*), presents a very different sequence, PxxxYAxFQ, in this region. Its peroxisomal location may account for this divergent evolution as compared to the mitochondrial carriers.

Along this line, it is interesting to consider the mitochondrial peripheral benzodiazepine receptor (TSPO/PBR), which contains a CRAC sequence (cholesterol recognition amino acid consensus), L/V-X(1−5)-Y-X(1−5)-R/K, in the cytosolic C-terminal region. NMR experiments combined with molecular modeling of a synthetic peptide corresponding to

the putative TM5 and C-terminal region of rat TSPO/PBR revealed a central patch of aromatic residues in the vicinity of the CRAC sequence (*42*). A girdle of three aromatic residues, Y152, Y153, and W155 in the transmembrane domain, builds up "a strong interfacial anchoring motif", two residues of which are essential for cholesterol binding (Y152 and Y153). The aromatic rings of these amino acids might constitute the gate of a groove in TM5 delineated by residues Y152, T148, and L144 on one side and Y153, M149, and A145 on the other side and where cholesterol, a planar molecule, might bind. However, determination of the cholesterol translocation pathway and of the distances between cholesterol and aromatic residue rings needs further investigation.

Also of interest is the bacterial nucleoside transporter Tsx whose crystal structure was obtained in the presence of nucleosides (*43*). Although its structure is more like that of a porin, Tsx presents well-defined binding sites for nucleosides. The Tsx pore is lined with eight aromatic residues, of which six are paired. The three pairs of aromatic residues are highly conserved among Tsx homologues. Two nucleosides are situated along the center of the channel consisting of the eight residues. The base moieties are stacked between aromatic residues, which also create van der Waals contacts with the sugar moieties. Therefore, involvement of a structural aromatic residue motif in substrate recognition and translocation is not restricted to the mitochondrial carrier family but might also involve proteins, whose substrates contain unsaturated chemical rings likely involved in stacking interactions with protein aromatic amino acids.

ACKNOWLEDGMENT

We thank Corinne Blancard for technical assistance. This paper is dedicated to the memory of Jean-Frédéric Sanchez who passed away in May 2008.

REFERENCES

1. Pebay-Peyroula, E., Dahout-Gonzalez, C., Kahn, R., Trézéguet, V., Lauquin, G. J.-M., and Brandolin, G. (2003) Structure of mitochondrial ADP/ATP carrier in complex with carboxyatractyloside. *Nature 426*, 39–44.
2. Fiore, C., Trézéguet, V., Le Saux, A., Roux, P., Schwimmer, C., Dianoux, A.-C., Noël, F., Lauquin, G. J.-M., Brandolin, G., and Vignais, P. V. (1998) The mitochondrial ADP/ATP carrier: structural, physiological and pathological aspects. *Biochimie 80*, 137–150.
3. Majima, E., Yamaguchi, N., Chuman, H., Shinohara, Y., Ishida, M., Goto, S., and Terada, H. (1998) Binding of the fluorescein derivative eosin Y to the mitochondrial ADP/ATP carrier: characterization of the adenine nucleotide binding site. *Biochemistry 37*, 424–432.
4. Pfaff, E., and Klingenberg, M. (1968) Adenine nucleotide translocation of mitochondria. 1. Specificity and control. *Eur. J. Biochem. 6*, 66–79.
5. Verdouw, H., and Bertina, R. M. (1973) Affinities of ATP for the dinitrophenol-induced ATPase. *Biochim. Biophys. Acta 325*, 385–396.
6. Kolarov, J., Kolarova, N., and Nelson, N. (1990) A third ADP/ATP translocator gene in yeast. *J. Biol. Chem. 265*, 12711–12716.
7. Pebay-Peyroula, E., and Brandolin, G. (2004) Nucleotide exchange in mitochondria: insight at a molecular level. *Curr. Opin. Struct. Biol. 14*, 420–425.
8. Nury, H., Dahout-Gonzalez, C., Trézéguet, V., Lauquin, G. J.-M., Brandolin, G., and Pebay-Peyroula, E. (2006) Relations between structure and function of the mitochondrial ADP/ATP carrier. *Annu. Rev. Biochem. 75*, 713–741.
9. Nelson, D. R., Lawson, J. E., Klingenberg, M., and Douglas, M. G. (1993) Site-directed mutagenesis of the yeast mitochondrial ADP/ATP translocator. Six arginines and one lysine are essential. *J. Mol. Biol. 230*, 1159–1170.
10. Müller, V., Basset, G., Nelson, D. R., and Klingenberg, M. (1996) Probing the role of positive residues in the ADP/ATP carrier from yeast. The effect of six arginine mutations on oxidative phosphorylation and AAC expression. *Biochemistry 35*, 16132–16143.
11. Müller, V., Heidkamper, D., Nelson, D. R., and Klingenberg, M. (1997) Mutagenesis of some positive and negative residues occurring in repeat triad residues in the ADP/ATP carrier from yeast. *Biochemistry 36*, 16008–16018.
12. Heidkamper, D., Müller, V., Nelson, D. R., and Klingenberg, M. (1996) Probing the role of positive residues in the ADP/ATP carrier from yeast. The effect of six arginine mutations on transport and the four ATP versus ADP exchange modes. *Biochemistry 35*, 16144–16152.
13. Marty, I., Brandolin, G., Gagnon, J., Brasseur, R., and Vignais, P. V. (1992) Topography of the membrane-bound ADP/ATP carrier assessed by enzymatic proteolysis. *Biochemistry 31*, 4058–4065.
14. Dahout-Gonzalez, C., Ramus, C., Dassa, E. P., Dianoux, A.-C., and Brandolin, G. (2005) Conformation-dependent swinging of the matrix loop m2 of the mitochondrial *Saccharomyces cerevisiae* ADP/ATP carrier. *Biochemistry 44*, 16310–16320.
15. Majima, E., Koike, H., Hong, Y. M., Shinohara, Y., and Terada, H. (1993) Characterization of cysteine residues of mitochondrial ADP/ATP carrier with the SH-reagents eosin 5-maleimide and N-ethylmaleimide. *J. Biol. Chem. 268*, 22181–22187.
16. Majima, E., Shinohara, Y., Yamaguchi, N., Hong, Y. M., and Terada, H. (1994) Importance of loops of mitochondrial ADP/ATP carrier for its transport activity deduced from reactivities of its cysteine residues with the sulfhydryl reagent eosin-5-maleimide. *Biochemistry 33*, 9530–9536.
17. Majima, E., Ikawa, K., Takeda, M., Hashimoto, M., Shinohara, Y., and Terada, H. (1995) Translocation of loops regulates transport activity of mitochondrial ADP/ATP carrier deduced from formation of a specific intermolecular disulfide bridge catalyzed by copper-o-phenanthroline. *J. Biol. Chem. 270*, 29548–29554.
18. Boulay, F., Lauquin, G. J.-M., Tsugita, A., and Vignais, P. V. (1983) Photolabeling approach to the study of the topography of the atractyloside binding site in mitochondrial adenosine 5′-diphosphate/adenosine 5′-triphosphate carrier protein. *Biochemistry 22*, 477–484.
19. Dalbon, P., Brandolin, G., Boulay, F., Hoppe, J., and Vignais, P. V. (1988) Mapping of the nucleotide-binding sites in the ADP/ATP carrier of beef heart mitochondria by photolabeling with 2-azido[alpha-^{32}P]adenosine diphosphate. *Biochemistry 27*, 5141–5149.
20. Dianoux, A.-C., Noël, F., Fiore, C., Trézéguet, V., Kieffer, S., Jaquinod, M., Lauquin, G. J.-M., and Brandolin, G. (2000) Two distinct regions of the yeast mitochondrial ADP/ATP carrier are photolabeled by a new ADP analogue: 2-azido-3′-*O*-naphthoyl-[beta-^{32}P]ADP. Identification of the binding segments by mass spectrometry. *Biochemistry 39*, 11477–11487.
21. Brandolin, G., Meyer, C., Defaye, G., Vignais, P. M., and Vignais, P. V. (1974) Partial purification of an atractyloside-binding protein from mitochondria. *FEBS Lett. 46*, 149–153.
22. Block, M. R., Lauquin, G. J.-M., and Vignais, P. V. (1982) Interaction of 3′-*O*-(1-naphthoyl)adenosine 5′-diphosphate, a fluorescent adenosine 5′-diphosphate analogue, with the adenosine 5′-diphosphate/adenosine 5′-triphosphate carrier protein in the mitochondrial membrane. *Biochemistry 21*, 5451–5457.
23. De Marcos Lousa, C., Trézéguet, V., Dianoux, A.-C., Brandolin, G., and Lauquin, G. J.-M. (2002) The human mitochondrial ADP/ATP carriers: kinetic properties and biogenesis of wild type and mutant proteins in the yeast *S. cerevisiae*. *Biochemistry 41*, 14412–14420.
24. Brandolin, G., Le Saux, A., Trézéguet, V., Vignais, P. V., and Lauquin, G. J.-M. (1993) Biochemical characterisation of the isolated Anc2 adenine nucleotide carrier from *Saccharomyces cerevisiae* mitochondria. *Biochem. Biophys. Res. Commun. 192*, 143–150.
25. Boeke, J. D., Trueheart, J., Natsoulis, G., and Fink, G. R. (1987) 5-Fluoroorotic acid as a selective agent in yeast molecular genetics. *Methods Enzymol. 154*, 164–175.
26. Chenna, R., Sugawara, H., Koike, T., Lopez, R., Gibson, T. J., Higgins, D. G., and Thompson, J. D. (2003) Multiple sequence alignment with the Clustal series of programs. *Nucleic Acids Res. 31*, 3497–3500.
27. Sali, A., and Blundell, T. L. (1993) Comparative modelling by satisfaction of spatial restraints. *J. Mol. Biol. 234*, 779–815.

28. Morris, G. M., Goodsell, D. S., Halliday, R. S., Huey, R., Hart, W. E., Belew, R. K., and Olson, A. J. (1998) Automated docking using a Lamarckian genetic algorithm and empirical binding free energy function. *J. Comput. Chem. 19*, 1639–1662.
29. Schuettelkopf, A. W., and van Aalten, D. M. F. (2004) PRODRG—a tool for high-throughput crystallography of protein-ligand complexes. *Acta Crystallogr. D60*, 1355–1363.
30. Sanner, M. F. (1999) Python: A programming language for software integration and development. *J. Mol. Graphics Mod. 17*, 57–61.
31. Brandolin, G., Boulay, F., Dalbon, P., and Vignais, P. V. (1989) Orientation of the N-terminal region of the membrane-bound ADP/ATP carrier protein explored by antipeptide antibodies and an arginine-specific endoprotease. Evidence that the accessibility of the N-terminal residues depends on the conformational state of the carrier. *Biochemistry 28*, 1093–1100.
32. Michejda, J., Guo, X. J., and Lauquin, G. J.-M. (1990) The respiration of cells and mitochondria of porin deficient yeast mutants is coupled. *Biochem. Biophys. Res. Commun. 171*, 354–361.
33. Postis, V., De Marcos Lousa, C., Arnou, B., Lauquin, G. J.-M., and Trézéguet, V. (2005) Subunits of the yeast mitochondrial ADP/ATP carrier: cooperation within the dimer. *Biochemistry 44*, 14732–14740.
34. Gallivan, J. P., and Dougherty, D. A. (1999) Cation-π interactions in structural biology. *Proc. Natl. Acad. Sci. U.S.A. 96*, 9459–9464.
35. Wang, Y., and Tajkhorshid, E. (2008) Electrostatic funneling of substrate in mitochondrial inner membrane carriers. *Proc. Natl. Acad. Sci. U.S.A. 105*, 9598–9603.
36. Dehez, F., Pebay-Peyroula, E., and Chipot, C. (2008) Binding of ADP in the mitochondrial ADP/ATP carrier is driven by an electrostatic funnel. *J. Am. Chem. Soc. 130*, 12725–12733.
37. Cavero, S., Traba, J., Del Arco, A., and Satrústegui, J. (2005) The calcium-dependent ATP-Mg/Pi mitochondrial carrier is a target of glucose-induced calcium signalling in *Saccharomyces cerevisiae*. *Biochem. J. 392*, 537–544.
38. Prohl, C., Pelzer, W., Diekert, K., Kmita, H., Bedekovics, T., Kispal, G., and Lill, R. (2001) The yeast mitochondrial carrier Leu5p and its human homologue Graves' disease protein are required for accumulation of coenzyme A in the matrix. *Mol. Cell. Biol. 21*, 1089–1097.
39. Vozza, A., Blanco, E., Palmieri, L., and Palmieri, F. (2004) Identification of the mitochondrial GTP/GDP transporter in *Saccharomyces cerevisiae*. *J. Biol. Chem. 279*, 20850–20857.
40. Marobbio, C. M., Di Noia, M. A., and Palmieri, F. (2006) Identification of a mitochondrial transporter for pyrimidine nucleotides in *Saccharomyces cerevisiae*: bacterial expression, reconstitution and functional characterization. *Biochem. J. 393*, 441–446.
41. Palmieri, L., Rottensteiner, H., Girzalsky, W., Scarcia, P., Palmieri, F., and Erdmann, R. (2001) Identification and functional reconstitution of the yeast peroxisomal adenine nucleotide transporter. *EMBO J. 20*, 5049–5059.
42. Jamin, N., Neumann, J. M., Ostuni, M. A., Vu, T. K., Yao, Z. X., Murail, S., Robert, J. C., Giatzakis, C., Papadopoulos, V., and Lacapère, J.-J. (2005) Characterization of the cholesterol recognition amino acid consensus sequence of the peripheral-type benzodiazepine receptor. *Mol. Endocrinol. 19*, 588–594.
43. Ye, J., and van den Berg, B. (2004) Crystal structure of the bacterial nucleoside transporter Tsx. *EMBO J.* 3187–3195.
44. Hatanaka, T., Kihira, Y., Shinohara, Y., Majima, E., and Terada, H. (2001) Characterization of loops of the yeast mitochondrial ADP/ATP carrier facing the cytosol by site-directed mutagenesis. *Biochem. Biophys. Res. Commun. 286*, 936–942.

BI8012565